THE JOURNAL OF BIOLOGICAL CHEMISTRY VOL. 284, NO. 3, pp. 1570–1582, January 16, 2009

Activity of the Neuronal Cold Sensor TRPM8 Is Regulated by Phospholipase C via the Phospholipid Phosphoinositol 4,5-Bisphosphate*[S]

Received for publication, September 19, 2008, and in revised form, November 18, 2008 Published, JBC Papers in Press, November 18, 2008, DOI 10.1074/jbc.M807270200

Richard L. Daniels[‡], Yoshio Takashima[‡], and David D. McKemy[‡§1]

From the [‡]Neuroscience Graduate Program, [§]Neurobiology Section, Department of Biological Sciences, University of Southern California, Los Angeles, California 90089

Cold temperatures robustly activate a small cohort of somatosensory nerves, yet during a prolonged cold stimulus their activity will decrease, or adapt, over time. This process allows for the discrimination of subtle changes in temperature. At the molecular level, cold is detected by transient receptor potential melastatin 8 (TRPM8), a nonselective cation channel expressed on a subset of peripheral afferent fibers. We and others have reported that TRPM8 channels also adapt in a calcium-dependent manner when activated by the cooling compound menthol. Additionally, TRPM8 activity is sensitive to the phospholipid phosphoinositol 4,5-bisphosphate (PIP_2), a substrate for the enzyme phospholipase C (PLC). These results suggest an adaptation model whereby TRPM8-mediated Ca^{2+} influx activates PLC, thereby decreasing PIP_2 levels and resulting in reduced TRPM8 activity. Here we tested this model using pharmacological activation of PLC and by manipulating PIP_2 levels independent of both PLC and Ca^{2+}. PLC activation leads to adaptation-like reductions in cold- or menthol-evoked TRPM8 currents in both heterologous and native cells. Moreover, PLC-independent reductions in PIP_2 had a similar effect on cold- and menthol-evoked currents. Mechanistically, either form of adaptation does not alter temperature sensitivity of TRPM8 but does lead to a change in channel gating. Our results show that adaptation is a shift in voltage dependence toward more positive potentials, reversing the trend toward negative potentials caused by agonist. These data suggest that PLC activity not only mediates adaptation to thermal stimuli, but likely underlies a more general mechanism that establishes the temperature sensitivity of somatosensory neurons.

The detection of temperature is a fundamental task of the nervous system. Temperature-sensing sensory afferent neurons reside in either the trigeminal (TG)[2] or dorsal root (DRG) sensory ganglia and project peripherally, terminating as free nerve endings that innervate areas of the head or trunk, respectively (1, 2). Subpopulations of these afferents respond to distinct sub-modalities of thermal stimuli, including noxious heat, innocuous cooling and warmth, and painfully cold temperatures. Each carries thermal information to the dorsal horn of the spinal cord, synapsing with neurons that project centrally (1, 3).

The discovery of thermosensitive ion channels of the transient receptor potential (TRP) family demonstrated an underlying molecular mechanism for temperature detection (4). Cold temperature sensation is largely mediated by TRPM8, a nonselective cation channel expressed on a small subset of neurons (5, 6). TRPM8 is activated by cooling compounds, such as menthol, as well as cold temperatures below ~28 °C, *in vitro* (7, 8). Recent reports on the behavioral phenotype of TRPM8-null mice suggest that this lone channel is required for the majority of cold sensing *in vivo* (5, 9–11). These and other data strongly implicate TRPM8 in not only the detection of both innocuous cool and some aspects of noxious cold but also injury-induced hypersensitivity to cold and, paradoxically, cooling-mediated analgesia (11, 12). Thus, understanding regulatory mechanisms that alter TRPM8 activity will provide keen insights into temperature sensation, nociception, and analgesia.

One fundamental property of cold-sensitive neurons is an intrinsic ability to adapt to prolonged cold stimuli, a mechanism that is likely critical for discrimination of changing environmental conditions (13, 14). We and others have shown that cold-sensitive neurons adapt to cold and menthol over time *in vitro* (6, 15), a phenomenon also observed with recombinant TRPM8 channels activated by menthol (7). During sustained exposure to menthol, TRPM8 currents adapt in a manner that is dependent upon the presence of external calcium (7). Interestingly, cold- and menthol-evoked currents are highly sensitive to cellular manipulation. In heterologous cells, TRPM8 currents quickly decrease or run down upon membrane patch excision (16, 17). Moreover, in membrane patches excised from cold- and menthol-sensitive DRG neurons, cold thresholds for current activation exhibit a shift of ~10 °C to colder tempera-

* This work was supported, in whole or in part, by National Institutes of Health Grant R01 NS054069 (NINDS) (to D. D. M.). The costs of publication of this article were defrayed in part by the payment of page charges. This article must therefore be hereby marked "*advertisement*" in accordance with 18 U.S.C. Section 1734 solely to indicate this fact.

[S] The on-line version of this article (available at http://www.jbc.org) contains supplemental Figs. 1 and 2.

[1] To whom correspondence should be addressed: 3641 Watt Way, HNB228, Los Angeles, CA 90089. Fax: 213-740-5687; E-mail: mckemy@usc.edu.

[2] The abbreviations used are: TG, trigeminal ganglia; PIP_2, phosphoinositol 4,5-bisphosphate; PLC, phospholipase C; TRP, transient receptor potential; TRPM8, transient receptor potential melastatin 8; PH, pleckstrin homology; FKBP, FK506-binding protein; GFP, green fluorescent protein; Inp54p, inositol-5-phosphate; IP_3, inositol trisphosphate; DRG, dorsal root ganglia; RFP, red fluorescent protein; YFP, yellow fluorescent protein; RT, reverse transcription; DAG, diacylglycerol; FBS, fetal bovine serum; EGFP, enhanced GFP; PKC, protein kinase C; BAPTA, 1,2-bis(2-aminophenoxy)ethane-*N*,*N*,*N*′,*N*′-tetraacetic acid.

tures in comparison with thresholds recorded in intact cells (18).

Phosphatidylinositol 4,5-bisphosphate (PIP_2) is a membrane phospholipid that accounts for ~1% of all lipids in the inner leaflet of the plasma membrane and is known to regulate a variety of ion channels, including TRPM8 (16, 17). When applied to the cytoplasmic face of excised membrane patches containing TRPM8 channels, PIP_2 can recover menthol-evoked currents to near pre-rundown levels (16, 17). PIP_2 is proposed to interact with channels either through electrostatic interactions or by binding to target proteins at specific phosphoinositide-binding sites (19, 20). Membrane PIP_2 levels are a product of enzymatic activity, such as phosphoinositide kinases that synthesize PIP_2 from membrane precursors and phospholipase C (PLC) that hydrolyzes it, creating membrane-bound diacylglycerol (DAG) and cytosolic inositol trisphosphate (IP_3), both of which function as second messengers. Of the three different PLC isotypes, PLCδ isoforms are modulated by increases in intracellular calcium (21).

When taken in context with the sensitivity of TRPM8 currents to PIP_2 levels, a model has been proposed whereby adaptation is a result of channel-mediated Ca^{2+} influx activating one or more PLCδ isoforms (16, 17). The subsequent reductions in PIP_2 levels then promote reduced or adapted TRPM8 currents. However, this hypothesis has not been conclusively shown in intact heterologous cells or in somatosensory neurons expressing TRPM8. Moreover, other alternative hypotheses for TRPM8 adaptation have been proposed, including Ca^{2+}-dependent kinase activity mediated by protein kinase C (22, 23). Thus, the cellular and molecular mechanisms for Ca^{2+}-mediated TRPM8 adaptation are unclear.

Here we show, in both heterologous cells and native TRPM8-expressing neurons, that Ca^{2+}-independent activation of PLC results in adapted TRPM8 currents. Moreover, PLC- and Ca^{2+}-independent PIP_2 depletion in heterologous cells produces similar effects on TRPM8 activity, again reducing both cold- and menthol-evoked currents. Mechanistically, we find that all such manipulations do not alter the temperature sensitivity of the channel but do lead to a shift in the voltage dependence of TRPM8 channel gating.

EXPERIMENTAL PROCEDURES

Oocyte Electrophysiology—Complementary RNA transcripts were injected into *Xenopus laevis* oocytes as described (7). Two-electrode voltage clamp recordings were performed 2–7 days after injection. Temperature ramps were generated by heating (35 °C) or cooling (4 °C) the perfusate in a Harvard coil and monitoring temperature changes with a thermistor placed near the oocyte.

Heterologous Expression—EGFP-Lyn-PH-PP was a kind gift from Tobias Meyer (Stanford University, Palo Alto, CA) and Mark S. Shapiro (University of Texas Health Science Center, San Antonio). PLCδ1-PH-RFP, PLCδ1-PH-YFP, and the components for inducible phosphatase translocation (FKBP-Inp54p and Lyn11-FRB) were kind gifts from Bertil Hille and Ken Mackie (University of Washington, Seattle) and Emily Liman (University of Southern California, Los Angeles). cDNA of TRPM8 clones and other molecules was transfected into the human embryonic kidney cell line 293 (HEK293T) using Lipofectamine 2000 (Invitrogen), as described (7) and following the manufacturer's instructions.

Mammalian Cell Electrophysiology—Voltage clamp recordings in neuronal and non-neuronal cells were performed as described (6, 7, 24). Standard bath solution for whole-cell recordings contained (in mM) 140 NaCl, 5 KCl, 1 $MgCl_2$, 2 $CaCl_2$, 10 HEPES, 10 glucose, and pH 7.4 (adjusted with NaOH). Pipette solution for whole-cell recordings contained (in mM) 140 CsCl, 0.5–5 EGTA, 2 MgATP, 10 HEPES, pH 7.4 (adjusted with CsOH). Nominally Ca^{2+}-free bath solutions contained (in mM) 140 NaCl, 5 KCl, 1 $MgCl_2$, 10 HEPES, 10 glucose, adjusted to pH 7.4 with NaOH. In some experiments 0.5 mM EGTA was added to this buffer. Recordings were performed using an Axopatch 200B amplifier (Molecular Devices, Inc., Sunnyvale, CA) and Digidata 1320 data acquisition board (Molecular Devices, Inc., Sunnydale, CA) with pCLAMP 9.2 software (Molecular Devices, Inc., Sunnyvale, CA). Solutions were exchanged by gravity fed tubes connected to an 8-channel perfusion valve solution controller (Warner Instruments, Hamden, CT) and fed into a recording chamber (Warner Instruments, Hamden, CT). The temperature of the perfusate was controlled by a Perfusion Temperature Controller RDTC-1 (Bioscience Tools, San Diego, CA). Bath temperature was recorded by a small thermocouple located in the recording chamber. Rapid solution exchange was performed as described (24). Briefly, in magnesium and calcium block experiments, rapid bath solution exchange was achieved by placing the cell in front of a linear array of microperfusion pipes under computer control (Warner Instruments, Hamden, CT). All drugs used in our experiments were stored and handled following the manufacturer's instructions.

Transgenic Mice—Transgenic mice expressing EGFP under control of the TRPM8 promoter were described previously (6). All animals were handled and cared for in accordance with guidelines established by the University of Southern California Animal Care and Use Committee.

Neuronal Cell Culture and Ca^{2+} Microfluorimetry—Trigeminal ganglia were dissected from newborn transgenic mice and dissociated with 0.25% collagenase P (Roche Applied Science) in a solution of 50% Dulbecco's modified Eagle's medium with 4.5 g/liter glucose, L-glutamine, and sodium pyruvate, Mediatech, Inc., Manassas, VA), and 50% F-12 (Ham's F-12 Nutrient Mixture with L-glutamine, Invitrogen) for 30 min. The ganglia were then pelleted and resuspended in 0.05% trypsin at 37 °C for 2 min, and triturated gently with a fire-polished Pasteur pipette in culture medium (Dulbecco's modified Eagle's medium/F-12 with 10% FBS and penicillin/streptomycin). Cells were then resuspended in culture medium with nerve growth factor 7S (Invitrogen) (100 ng/ml) and plated onto coverslips coated with Matrigel (BD Biosciences) (20 μl/ml). Cultures were examined 16–20 h after plating. Intracellular Ca^{2+} was determined with the cell-permeable form of Fura-2 (Invitrogen) as described (7), and pseudo-colored ratiometric images were captured on an Olympus IX70 fluorescent microscope with Sutter Lambda LS light source, Roper CoolSnap ES camera, and the MetaImaging software suite. Confocal images were

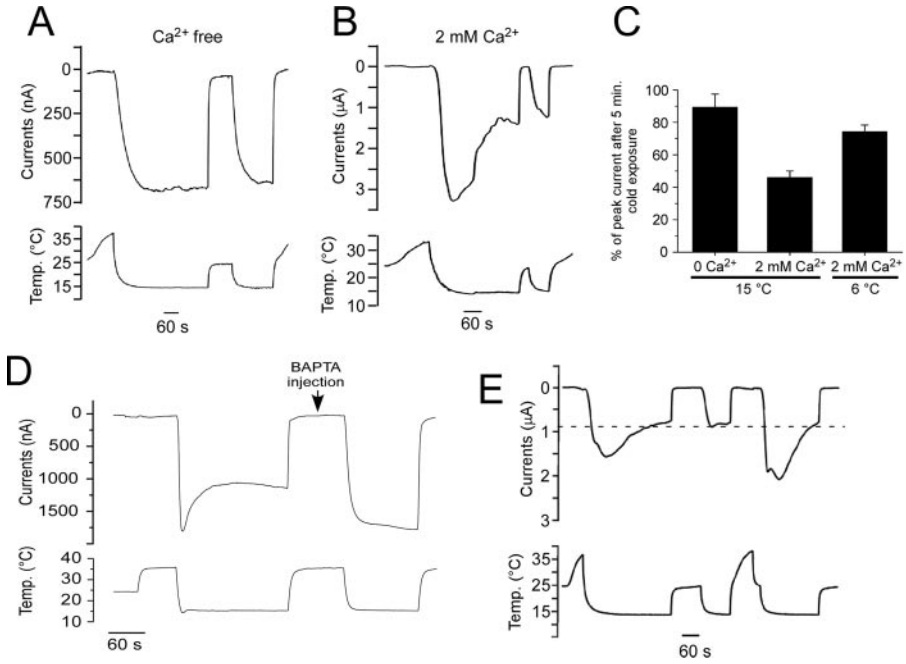

FIGURE 1. **Adaptation of cold-evoked TRPM8 currents is dependent upon calcium and temperature.** *A*, in two-electrode voltage clamp recordings from rTRPM8-expressing *Xenopus* oocytes, cooling of nominally Ca^{2+}-free bath solutions to 15 °C evokes robust inward currents (holding potential of −60 mV) that are sustained for the duration of the cold stimulus (5 min). Warming of the perfusate to room temperature inhibited these currents, but a second cold ramp returned currents to previous levels ($n = 5$). *B*, in the presence of physiological (2 mM) Ca^{2+}, a cold ramp to 15 °C also produces robust inward currents, yet these decrease over time, and subsequent cold stimuli evoke smaller, adapted currents ($n = 4$). *C*, TRPM8 adaptation is dependent upon temperature. In the presence of 2 mM external Ca^{2+}, currents adapt more readily to moderately cool temperatures (15 °C) than strong cold pulses (6 °C) in the presence of 2 mM Ca^{2+} ($n = 3$–6). *D*, before BAPTA injection, cold-evoked inward currents adapt in the presence of 2 mM external Ca^{2+}. After BAPTA injection (50 μl of a 100 mM solution), cold-evoked currents do not adapt ($n = 4$). *E*, prolonged cold stimulus (15 °C) in the presence of 2 mM Ca^{2+} produces robust and adapting inward currents, which remain at adapted current magnitudes (*dashed line*) until the bath solution is brought to physiological temperatures (>30 °C).

collected on a Zeiss LSM510 confocal microscope and analyzed with MetaMorph software. Acquired fluorescent images are shown in negative contrast such that fluorescence is represented as dark.

Fluorescence-activated Cell Sorting and RT-PCR—Freshly dispersed TG neurons (prepared as described above) were sorted by GFP fluorescence with a MoFlo Cytomation Cell Sorter, and total RNA was purified using the Qiagen RNeasy kit following the manufacturer's instructions. The presence of PLCδ isozymes was determined by RT-PCR with the Qiagen One-step RT-PCR kit following the manufacturer's instructions. Primers for each isozyme were as follows: PLCδ1 forward, 5′-GGCAGGCATTCTATGAGATG-3′, and reverse, 5′-GGGGTCCACGATAGAATTCT-3′; PLCδ3 forward, 5′-TCAGGTTTGTGGTAGAAGAT-3′, and reverse, 5′-TTCCTCTTCGGTCTTTTCAG-3′; PLCδ4 forward, 5′-CCATCATGTGCCCAGACCTA-3′, and reverse, 5′-TCCATCCCACATAACCGGTT-5′; and TRPM8 forward, GCTCTCCACCAATATCCTTC-3′, and reverse, 5′-CAGTAGGTGGGACACGAGTC-3′.

Data Analysis—Data analysis was performed using Origin 6.1 (OriginLab Corp., Northampton, MA). Steady-state activation curves were determined using methods described previously (25, 26). Briefly, to estimate maximal TRPM8 activity at a given voltage, we used a saturating dose of 1 mM menthol at room temperature to activate TRPM8 and measured currents at the end of each voltage step. We then calculated the conductance, g, at each data point, using the relation $g = I_{ss}/V$, where I_{ss} is the steady-state current at the end of a voltage step, and V is the voltage difference across the cell membrane. Because the conductance appears to saturate and reach a maximum, we calculated g/g_{max} for each value, thus normalizing data so that comparisons could be made between cells. We assume for our calculations a two-state model of channel gating. Therefore, as in Refs. 25, 26, we fit the g/g_{max} values with steady-state activation curves using a Boltzmann function of the form shown in Equation 1,

$$g/g_{max} = \frac{1}{1 + \exp\left(-\frac{z_{app}}{k_B T}(V - V_{1/2})\right)} \quad \text{(Eq. 1)}$$

where z_{app} is the experimentally determined gating charge; k_B is the Boltzmann constant (1.38×10^{-23} J K^{-1}), and T is the absolute temperature. The half-maximal conductance ($V_{½}$) is estimated from these steady-state activation curves for each cell. Data are represented as the mean ± S.E. Statistical significance was assayed using a Student's t test.

RESULTS

Ca^{2+} Dependence of Cold-evoked TRPM8 Currents—Cold-evoked membrane currents, recorded in menthol-sensitive DRG neurons in primary culture, are reported to adapt in a Ca^{2+}-dependent manner (15). Moreover, in heterologous cells, we have shown that menthol-evoked TRPM8 currents adapt to prolonged menthol exposure only in the presence of external physiological Ca^{2+} (7). We set out to determine whether TRPM8 currents adapt to a cold stimulus like that observed in native cells. Using two-electrode voltage clamp recordings in rat TRPM8-expressing *Xenopus* oocytes, bathed in nominally free Ca^{2+} solutions, a cold ramp from ~32 to 15 °C evoked a rapid and reproducible inward current that was sustained for the length of the stimulus (Fig. 1*A*). In the presence of 2 mM external Ca^{2+}, cold-evoked (15 °C) currents were activated likewise, but then adapted to approximately half the peak values after 5 min (46.0 ± 4.1%, $n = 4$; Fig. 1, *B* and *C*). The degree of adaption was temperature-dependent as less adaption was observed if the perfusate was reduced to colder temperatures (6 °C, 74.3 ± 4.0%, $n = 3$; Fig. 1*C*). We also found that calcium exerts its effects on TRPM8 activity intracellularly. Even in the presence of 2 mM external Ca^{2+}, no adaption to cold was observed

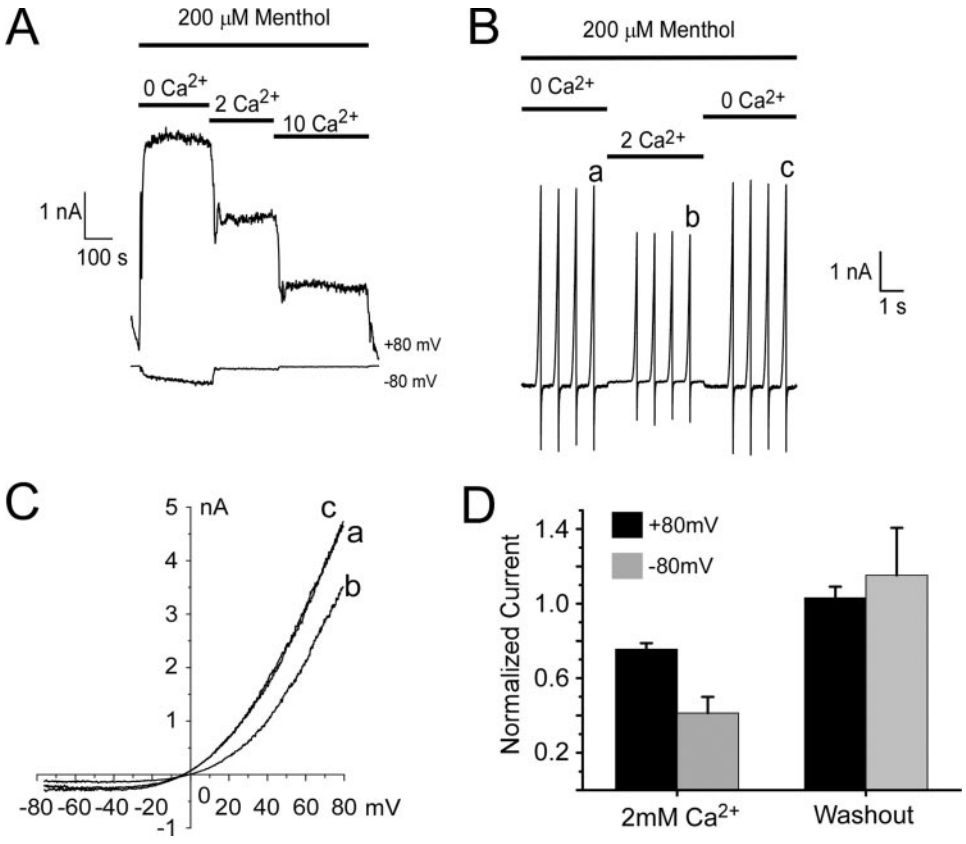

FIGURE 2. **Ca^{2+} acts as a channel blocker of TRPM8.** *A,* representative whole-cell voltage clamp recordings of TRPM8-expressing HEK293T cells show reduced menthol-evoked currents at both positive and negative membrane potentials as intracellular Ca^{2+} is increased. *B,* in the presence of 200 μM menthol, rapid solution exchange (<2 s) from nominally Ca^{2+}-free to 2 mM Ca^{2+} blocks TRPM8 currents measured during membrane voltage ramps from −80 to +80 mV. Of note, this divalent block was rapidly reversible as well. *C,* current-voltage relations from time points indicated in *B*. *D,* mean remaining currents are reduced by 41.3 ± 8.7% at positive potentials and 75.5 ± 4.9 at negative potentials ($n = 5$).

once intracellular Ca^{2+} was buffered by injection of the rapid Ca^{2+} chelator BAPTA into the oocyte (27) ($n = 4$; Fig. 1*D*). Finally, recovery from adaptation was found to be temperature-dependent as the magnitude of TRPM8 currents remained at the adapted levels as long as bath temperatures were held in the sub-physiological range (~22 °C). However, current amplitudes returned to pre-adapted levels once temperatures were raised above 30 °C (Fig. 1*E*). Thus, as in menthol-sensitive DRG neurons, cold-evoked TRPM8 currents adapt in a Ca^{2+}-dependent manner, yet remain adapted until temperatures are returned to physiological levels. These results suggest that TRPM8 adaptation is a Ca^{2+}- and temperature-dependent process.

Ca^{2+} and Other Divalent Cations Are TRPM8 Channel Blockers—We set out to determine the Ca^{2+}-dependent mechanisms that promote TRPM8 adaptation. However, it has been reported that TRPM8 currents are partially blocked by calcium and barium ions (28). Thus, it is critical to distinguish between physical blockade of the channel and decreased channel activity by other regulatory mechanisms, such as adaptation. To this end, we used whole-cell voltage clamp recordings of HEK293T cells expressing rat TRPM8 (7) in which the pipette solution contained 5 mM EGTA to buffer cytoplasmic Ca^{2+} and thus prevent adaptation. Under these conditions, we observed that external calcium reduced menthol-evoked currents in a concentration-dependent manner (Fig. 2*A*). To distinguish between block and adaptation, we employed a rapid perfusion system in which the external Ca^{2+} concentration was changed in less than 2 s (24). Quickly switching the perfusate from nominally Ca^{2+} free to 2 mM Ca^{2+} resulted in reduced menthol-evoked whole-cell currents, measured during voltage ramps from −80 to +80 mV (by 41.3 ± 8.7% at +80 mV and 75.5 ± 4.9% at −80 mV, $n = 5$), that recovered upon Ca^{2+} washout (Fig. 2, *B–D*). External magnesium also reversibly blocked menthol currents (not shown). Thus, with the rapid time course in the reduction of TRPM8 currents, and as intracellular Ca^{2+} was strongly buffered, it is unlikely that this effect was because of adaptation but is a result of block by Ca^{2+}. Therefore, in all subsequent experiments calcium concentration was held constant such that Ca^{2+} block was not misinterpreted as adaptation.

Chemical Activation of PLC Reduces Menthol-evoked TRPM8 Currents—Several groups have reported that PIP_2 levels effect TRPM8 activity in membrane patches excised from heterologous cells (16, 17, 29). These data, along with our previous results on the Ca^{2+} and temperature dependence of adaptation, suggest that PLC activation and subsequent PIP_2 hydrolysis induces adaptation, presumably through a rise in intracellular calcium via TRPM8. For adaptation to be mediated in this manner, menthol-evoked increases in intracellular Ca^{2+} must give rise to increased PLC activity. We tested if this was indeed the case in rTRPM8 transfected HEK293T cells using an optical probe that monitors depletion of PIP_2 (30). We used the PIP_2 reporter PH-PLCδ1 (a kind gift of reagents from B. Hille and K. Mackie), a fusion protein of red fluorescent protein (RFP) or yellow fluorescent protein (YFP), and the PIP_2- and IP_3-binding pleckstrin homology (PH) domain of PLCδ1, and we co-transfected it with TRPM8 in HEK293T cells. Under basal conditions, the majority of PH-PLCδ1 is bound to PIP_2 and localized to the plasma membrane (Fig. 3*A* and supplemental Fig. 1). We first confirmed that Ca^{2+} influx itself can promote translocation of the reporter from the membrane to the cytosol by applying 10 μM ionomycin to PH-PLCδ1-expressing HEK293T in the presence of 2 mM external Ca^{2+} (supplemental Fig. 1*A*). Next, we tested if Ca^{2+} influx via TRPM8 can likewise evoke translocation by applying 200 μM menthol in 2 mM external Ca^{2+}. As shown in Fig. 3, *A* and *B*, we observed increased cytosolic fluorescence, with a concomitant decrease in membrane fluorescence, indicating cleavage of PIP_2 (decrease at the membrane) and generation of

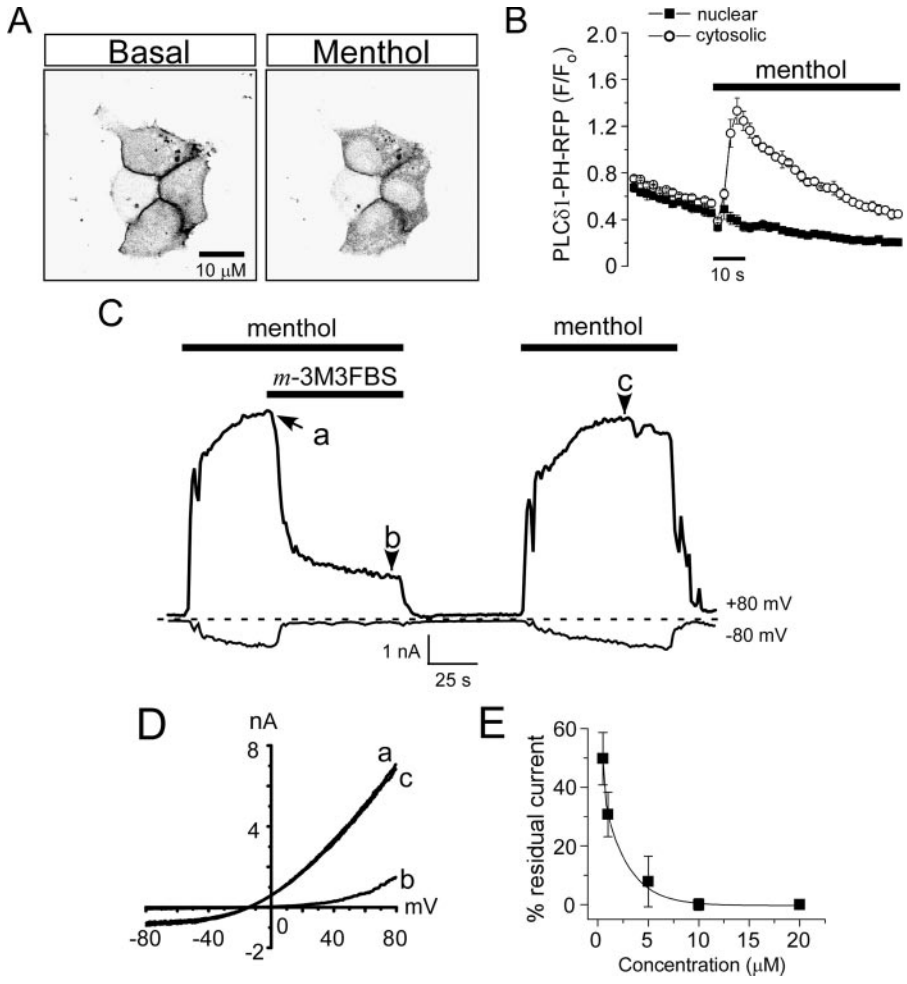

FIGURE 3. **Direct pharmacological activation of PLC by *m*-3M3FBS reduces menthol-evoked TRPM8 currents.** *A,* representative confocal images of menthol-evoked translocation of a PLCδ1-PH-RFP domain fusion protein reporter in the presence of 2 mM external Ca^{2+}. HEK293T cells were co-transfected with rTRPM8 and PLCδ-PH-RFP constructs, and RFP fluorescence was monitored before and after addition of 200 μM menthol to the bath solution (data representative of 10 independent experiments). Cells are shown in negative contrast. *B,* RFP fluorescence increased in the cytosol (*circles*) but remained constant in the nucleus (*boxes*) when the cells were exposed to 200 μM menthol. Data values are arbitrary fluorescence units (*F*) normalized to basal fluorescence (F_o). *C,* representative whole-cell voltage clamp recording from an rTRPM8-expressing HEK293T cell. Menthol-evoked currents (200 μM) were rapidly reduced upon bath co-application of 5 μM *m*-3M3FBS at both positive and negative membrane potentials. *D,* representative current-voltage relationships for menthol-evoked responses before (*a*), during (*b*), and after PLC activation (*c*). Data corresponds to the points in the recording indicated in *C*. *E,* reduction of TRPM8 currents by *m*-3M3FBS is dose-dependent. Each dosage was tested on 3–6 cells, and bars represent the means ± S.E.

IP_3 (increase in the cytosol). These data are consistent with a FRET-based approach that showed that menthol application can induce PH domain translocation in TRPM8-expressing COS-1 cells (17) and show that Ca^{2+} entry through TRPM8 is sufficient to increase PLC activity in HEK293T cells as well. When menthol was applied in nominally Ca^{2+}-free conditions, little change occurred in the localization of PH-PLCδ1 fluorescence (not shown).

Next, we sought to test the hypothesis that PLC regulates TRPM8 activity using the benzenesulfonamide compound *m*-3M3FBS, which activates all isoforms of PLC, including those of the calcium-sensitive PLCδ family (30–33). Thus, if adaptation is a result of Ca^{2+}-mediated activation of PLC, then PLC activation in the absence of a rise in intracellular Ca^{2+} should lead to reduced TRPM8 activity. We first tested the effectiveness of *m*-3M3FBS to activate PLC using the PH-PLCδ1 optical reporter. It has been previously reported that application of *m*-3M3FBS to heterologous cells expressing PH-PLCδ1 induces translocation of the reporter from the membrane to the cytosol (30), a finding that we reproduced in our HEK293T cells (supplemental Fig. 1*B*).

Next, we tested our hypothesis first by examining the effects of *m*-3M3FBS on menthol-evoked whole-cell TRPM8 currents in transiently transfected HEK293T cells recorded in Ca^{2+}-free conditions (nominally Ca^{2+} free external solutions and 5 mM EGTA in the pipette). At both positive and negative membrane potentials, 200 μM menthol-evoked robust inward currents that were strongly reduced after the addition of 5 μM *m*-3M3FBS when recorded at room temperature (Fig. 3, *C* and *D*, $n = 8$). Menthol-evoked currents were reduced by *m*-3M3FBS in a concentration-dependent manner, with effects starting as low as 1 μM and saturating at 10 μM, where little or no TRPM8 currents remained even after washout (Fig. 3*E*, $n = 8$). However, when the concentration of *m*-3M3FBS was kept at 5 μM or below, menthol currents were typically restored upon washout at positive membrane potentials, but rarely at negative potentials (Fig. 3, *C* and *D*). Because of the negligible amount of inward currents at negative membrane potentials, the rest of our analyses of channel function was recorded at positive membrane potentials.

Chemical Activation of PLC Reduces Cold-evoked TRPM8 Currents—We next tested if chemical activation of PLC has similar effects on cold-evoked TRPM8 currents in heterologous cells. In the absence of external Ca^{2+} and with Ca^{2+}-buffered pipette solutions, we first tested the effect of *m*-3M3FBS on sustained cold-evoked currents, measuring responses to a cold ramp from 32 to 17 °C. As shown previously, cold-evoked currents were maintained with persistent cold stimuli but were significantly reduced upon application of 5 μM *m*-3M3FBS ($n = 6$; Fig. 4, *A* and *B*). Moreover, the concentration dependence of the *m*-3M3FBS-induced reductions of cold currents was consistent with those observed for menthol-evoked currents (see Fig. 3*E* and supplemental Fig. 2*A*).

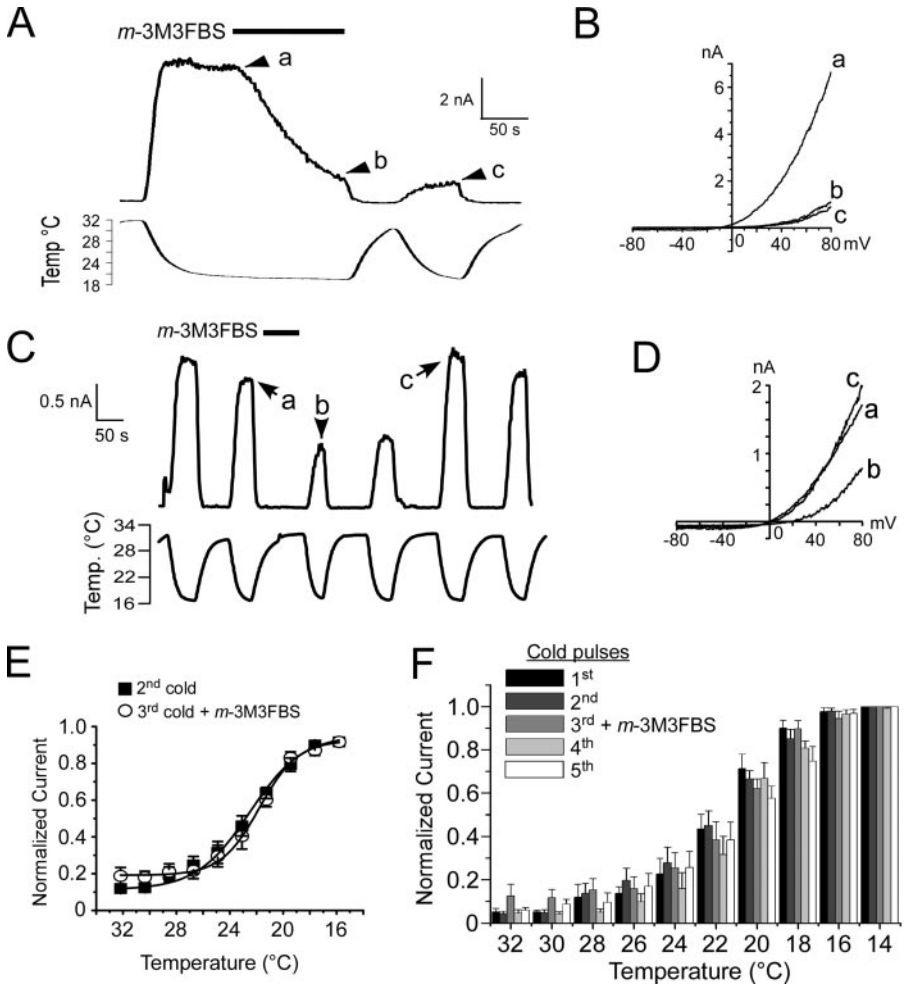

FIGURE 4. *A,* direct pharmacological activation of PLC reduces cold-evoked TRPM8 currents in heterologous cells. A cold ramp (from 32 to 19 °C) evoked robust membrane currents (at +80 mV) that were reduced upon application of 2.5 μM *m*-3M3FBS. In this cell, a subsequent cold pulse was reduced compared with the initial values. *B,* current-voltage relations obtained from the points indicated in *A*. *C,* representative whole-cell voltage clamp recording of TRPM8 cold currents evoked by successive cold ramps from 32 to 17 °C (holding potential (*h.p.*) +80 mV). When 2.5 μM *m*-3M3FBS was applied between the 2nd and 3rd cold pulses, cold-evoked TRPM8 currents were reduced but returned to their previous amplitudes with time. *D,* representative current-voltage relations of cold-evoked responses taken from the points indicated in the recording in *C*. *E,* current to temperature relationship of TRPM8 responses before and after activation of PLC by *m*-3M3FBS. Cold-evoked TRPM8 currents (in the presence of 50 μM menthol) were normalized to a maximal saturating response at 14 °C ($n = 6$). *F,* current to temperature relationship of cold-evoked TRPM8 responses across five successive temperature pulses. Data presented are the average normalized temperature response for each of the five consecutive cold pulses, and 2.5 μM *m*-3M3FBS was applied between the 2nd and 3rd cold pulses ($n = 6$).

Next we tested the effect of application of the PLC activator between consecutive cold pulses (from 32 to 14 °C) in a Ca^{2+}-free setting. To enhance cold-evoked currents, 50 μM menthol was included in the bath solution. Under these conditions, there was a slight reduction in current amplitude, recorded at positive membrane potentials, between the 1st and 2nd cold stimulus (decrease of 11.4 ± 3.9%, $n = 10$; Fig. 4*C*). However, all subsequent cold pulses evoked similar current amplitudes (98.0 ± 6.9%, amplitude of 3rd cold pulse as a percentage of the 2nd cold pulse, $n = 6$). Thus, we tested the effect of transient application of *m*-3M3FBS between the 2nd and 3rd cold pulses and found that directly activating PLC significantly reduced the current amplitude of cold-evoked currents (55.8 ± 8.5%, $n = 6$, $p < 0.01$, amplitude of 3rd cold pulse as a percentage of the 2nd cold pulse, see Fig. 4, *C* and *D*). As with menthol-evoked currents, cold currents were recovered to basal levels when *m*-3M3FBS was held at minimal concentrations (Fig. 4, *C* and *D*). Thus, in heterologous cells, direct activation of PLC in a manner independent of Ca^{2+} adapts TRPM8 currents similar to classical Ca^{2+}-mediated adaptation and supports the hypothesis that adaptation is a PLC-mediated process.

PLC Activation Does Not Shift the Temperature Sensitivity of TRPM8—Our data show that direct activation of PLC leads to a decrease in either cold- or menthol-evoked TRPM8 currents. However, it is not clear mechanistically how channel properties are altered under these conditions. One possible mechanism is that adaptation leads to a shift in the temperature dependence of TRPM8. Thus, adaption results because of a decrease in TRPM8 temperature sensitivity such that colder temperatures would be required to generate pre-adapted currents. Indeed, adaptation in other sensory systems has been shown to be manifested as a result in decreased sensitivity to sensory stimuli (34).

We first tested this premise by measuring the temperature dependence of TRPM8 currents before and after activation of PLC by *m*-3M3FBS. A five-cold pulse protocol was employed, where we applied 2.5 μM *m*-3M3FBS between the 2nd and 3rd cold pulses and examined the temperature dependence profiles by normalizing these responses to the peak currents recorded at 14 °C. With this approach, we found that the temperature dependence of cold-evoked currents before and after PLC activation was unchanged (Fig. 4*E*). We quantified temperature thresholds as the bath temperature where currents increased to 20% of the maximal, finding thresholds of 24.6 ± 1.2 and 22.9 ± 0.8 °C before and after PLC activation, respectively ($n = 5$). Moreover, when normalized cold-evoked currents were compared across all five cold ramps, there were no significant differences in their temperature dependences (Fig. 4*F*). Thus, although direct activation of PLC leads a reduction in TRPM8 activity, the effect is not manifested as a change in channel sensitivity to temperature.

PIP_2 Depletion in Intact Cells Reduces Menthol-evoked TRPM8 Currents—Mechanistically, the ability of PLC to regulate TRPM8 further supports data suggesting that channel

activity is highly sensitive to the content of the PIP_2 in the inner leaflet of the plasma membrane. Indeed, it has been shown that in inside-out oocyte membrane macropatches containing TRPM8, addition of PIP_2 to the cytosolic face, is sufficient to restore the rundown of TRPM8 currents that occurs upon patch excision (16, 17). However, in these studies the effect of PIP_2 on channel activity was recorded in isolated membrane patches and not in intact cells. Thus, it remains a possibility that it is not PIP_2 *per se* but rather the metabolic by-products of PIP_2 hydrolysis that regulates TRPM8 via their downstream effectors. Indeed, it has been reported that PKC-mediated phosphorylation is responsible for TRPM8 adaptation, although the channel does not appear to be a substrate for PKC (22, 23). Thus, we set out to determine whether PLC-independent reductions in PIP_2 in intact cells, without the production of diacylglycerol (DAG) or IP_3, affects menthol and cold-evoked currents.

We co-transfected HEK293T cells with TRPM8 and the membrane-tethered PIP_2-specific 5′-phosphatase Inp54p (construct Lyn-PH-PP-GFP; a gift from T. Meyer and M. Shapiro) (35, 36). This phospholipid phosphatase is expressed as a fusion protein with the myristoylation/palmitoylation region of the tyrosine kinase Lyn, thereby localizing to the plasma membrane and selectively reducing plasmalemmal PIP_2, but not other intracellular pools. Moreover, as this is a GFP fusion protein, cells expressing the phospholipid phosphatase are easily visualized (Fig. 5*A*). We initially used Ca^{2+} microfluorimetry with the intracellular Ca^{2+} indicator Fura-2 to compare menthol-evoked responses in TRPM8-expressing cells to those expressing both channel and the phosphatase (Fig. 5, *A* and *B*). Under these transfection conditions, cells were co-expressing Lyn-PH-PP-GFP and rTRPM8 (menthol-sensitive and GFP-positive; Fig. 5*A*, *green arrowheads*) or TRPM8 alone (menthol-sensitive; Fig. 5*A*, *red arrowheads*). Thus, with this approach, cells with reduced plasmalemmal PIP_2 were assayed alongside cells with basal PIP_2 content. We found that all cells in which menthol evoked a robust increase in intracellular Ca^{2+} were negative for GFP (0/177 cells), whereas those expressing the GFP fusion protein were either unresponsive or had a significantly reduced response to menthol (Fig. 5*C*; *peak R* at 200 μM menthol. 0.92 ± 0.01 *versus* 0.41 ± 0.02 for GFP^- *versus* GFP^+, respectively ($p < 0.01$)). Thus, these data suggest that cellular manipulations that decrease plasmalemmal PIP_2 in a PLC-independent manner reduce TRPM8 responsiveness to menthol.

One caveat for this approach is that phosphatase-expressing cells are operating with reduced PIP_2 levels for extended periods of time, thus potentially altering other cell functions that may indirectly affect TRPM8. Thus, we measured TRPM8 currents in cells in which we conditionally depleted plasmalemmal PIP_2 levels (37), an approach that has been reported to inhibit menthol-evoked currents in TRPM8-expressing heterologous cells (38). This system is advantageous because it provides a way to inducibly bring the PIP_2 5′-phosphatase Inp54p to the cell membrane by the addition of the dimerizing immunosuppressant rapamycin. The addition of rapamycin dimerizes the phosphatase FKBP-Inp54p (expressed as fusion protein with the FK506-binding protein (FKBP) and the fluorophore mCherry) with a membrane-anchored FKBP-rapamycin-binding domain

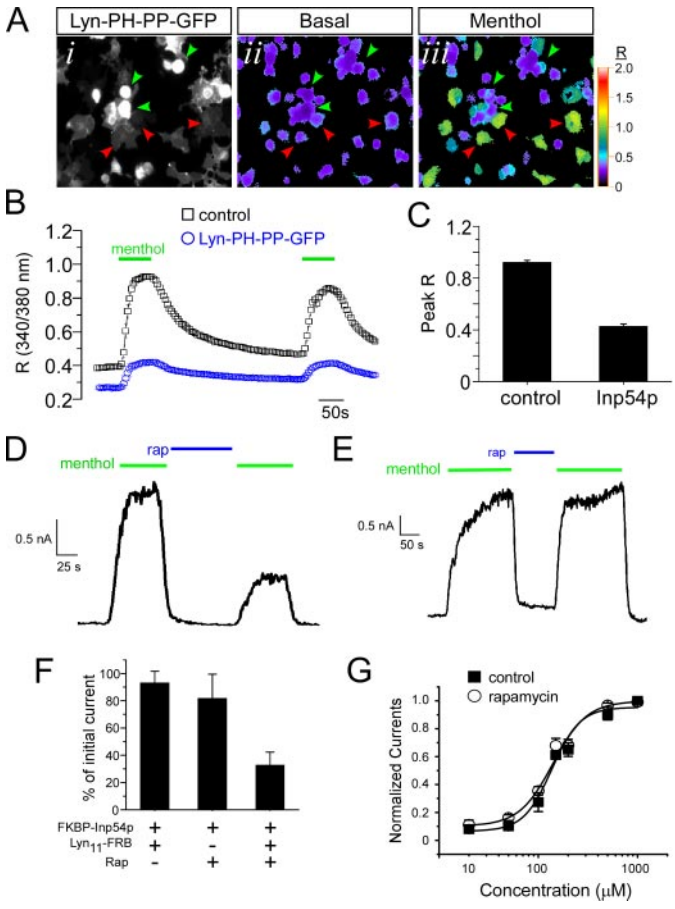

FIGURE 5. **PLC-independent depletion of plasmalemmal PIP_2 reduces menthol-evoked TRPM8 currents.** *A,* representative images of HEK293T cells expressing rTRPM8 and Lyn-PH-PP-GFP. *A, panel i*, GFP fluorescence marks the cells expressing both constructs and have reduced PIP_2 levels. Pseudocolored images of the 340/380 nm Fura-2 ratio show low basal Ca^{2+} before application of 200 μM menthol (*A, panel ii*). *Green arrowheads* mark GFP^+ cells expressing Lyn-PH-PP-GFP in which menthol evoked a small increase in *R* values, and *red arrowheads* mark GFP-negative cells in which menthol evoked a robust change in intracellular Ca^{2+} (*A, panel iii*). *B,* averaged changes in the Fura-2 ratio of control TRPM8-expressing cells (*black boxes*, $n = 20$ cells) *versus* those co-expressing Lyn-PH-PP-GFP (*blue circles*, $n = 25$ cells). *C,* average peak ratio values (1st menthol application) of individual cells and data are averaged responses from four independent experiments and 15–25 cells per experiment. *D,* representative whole-cell voltage clamp recording (holding potential (*h.p.*) +80 mV) from a cell transfected with rTRPM8, FKBP-Inp54p, and Lyn11-FRB. Menthol-evoked (200 μM) TRPM8 currents were diminished following application of the dimerizing agent rapamycin that translocates Inp54p to the membrane. *E,* whole-cell voltage clamp recording from a cell transfected with rTRPM8 and FKBP-Inp54p but not the membrane tethered component Lyn11-FRB. Repeated menthol-evoked (200 μM) TRPM8 currents did not diminish upon application of the dimerizer rapamycin. *F,* summary data of the reductions in menthol-evoked TRPM8 currents using the rapamycin (*Rap*), Inp54p translocation system ($n = 5$ cells for each condition). *G,* menthol dose-response relationship before and after rapamycin-induced Inp54p translocation and reduction of TRPM8 currents ($n = 3$–9 cells per menthol concentration).

(Lyn_{11}-FRB), thereby translocating the phosphatase to the membrane. We found that addition of 1 μM rapamycin reduced whole-cell menthol-evoked TRPM8 currents when FKBP-Inp54p and Lyn_{11}-FRB were co-expressed with TRPM8 (Fig. 5*D*). These data are consistent with our Ca^{2+} microfluorimetry results with the expression of membrane-bound Inp54p. At positive potentials, menthol currents were reduced to 36.8 ± 11.3% (Fig. 5*F*, $n = 5$) of their original magnitude, although at negative potentials, rapamycin effectively eliminated TRPM8

currents such that it excluded further evaluation (see supplemental Fig. 2*B*). Moreover, this effect was dependent upon translocation of Inp54p to the membrane as in cells containing phosphatase only (without the membrane-bound Lyn_{11}-FRB), the addition of rapamycin had no effect (Fig. 5, *E* and *F*, also see supplemental Fig. 2*C*). Finally, reductions in TRPM8 activity required dimerization as repeated menthol-evoked currents were unchanged in the presence of both components of the translocation system (Fig. 5*F*).

With reduced menthol responses after the dephosphorylation of PIP_2 by the 5′-phosphatase, we sought to determine whether changes in TRPM8 menthol sensitivity underlie this effect. Thus, we generated menthol dose-response relationships before and after the addition of rapamycin in HEK293T cells expressing TRPM8 and the translocation constituents. As shown in Fig. 5*G*, phosphatase-mediated reductions in PIP_2 levels did not significantly alter menthol sensitivity of TRPM8. The EC_{50} value of menthol-evoked currents before and after the translocation of Inp54p were 144.4 ± 15.2 μM and 135.4 ± 15.0 μM (n = 3–9 cells per menthol dose), respectively. Thus, reducing PIP_2 levels in intact cells does not alter menthol sensitivity of TRPM8.

PIP_2 Depletion Reduces Cold-evoked TRPM8 Currents without Altering Temperature Sensitivity—We also examined the temperature dependence of cold-evoked Ca^{2+} responses when PIP_2 levels were reduced. We co-expressed TRPM8 with membrane-bound Inp54p (Lyn-PH-PP-GFP) and compared cold-evoked Ca^{2+} responses as done previously for menthol (see Fig. 5). In cells expressing TRPM8 alone, rapid reductions in the temperature of the perfusate from 32 to 17 °C evoked a robust and reproducible increase in intracellular Ca^{2+} (Fig. 6, *A* and *B*). Similar responses were observed in cells co-expressing TRPM8 and Inp54p, but the magnitude of the Ca^{2+} response was significantly reduced to 59% of the TRPM8-alone cells (R_{TRPM8} = 2.9 ± 0.2, $R_{TRPM8\ +\ Inp54p}$ = 1.7 ± 0.2, n = 6 experiments, 25–57 cells per experiment, $p < 0.01$; Fig. 6*C*). However, when Ca^{2+} responses were normalized to peak values at 17 °C under these two conditions, there was no difference in temperature sensitivity (Fig. 6*D*). Apparent temperature thresholds (measured as the temperature where R increased by 15% above base line) were found to be 26.6 ± 0.8 °C (n = 57 cells) for TRPM8-expressing cells and 26.5 ± 1.4 °C (n = 49 cells) for TRPM8- and Inp54p-expressing cells.

We also used whole-cell voltage clamp recordings and the rapamycin-Inp54p translocation system to measure the temperature dependence of TRPM8 currents before and after phosphatase translocation. First, we established for the first time that addition of rapamycin in cells expressing TRPM8 and all the translocation components results in a reduction of cold-evoked TRPM8 currents (Fig. 6, *E* and *F*). As previously, we employed a multiple cold ramp protocol (from 30 to 14 °C) and applied rapamycin between the 2nd and 3rd cold pulses, observing that Inp54p translocation reduced TRPM8 cold-evoked currents to 60.6 ± 4.0% (n = 7) of their original magnitude. These data are consistent with the effects of Inp54p activity on menthol-evoked TRPM8 currents.

To determine the effect of PIP_2 depletion on the temperature dependence of TRPM8 currents, we plotted normalized cold-evoked currents to the peak currents recorded at 14 °C, at positive membrane potentials, obtained during the 2nd and 3rd (after rapamycin) cold ramps. As shown in Fig.

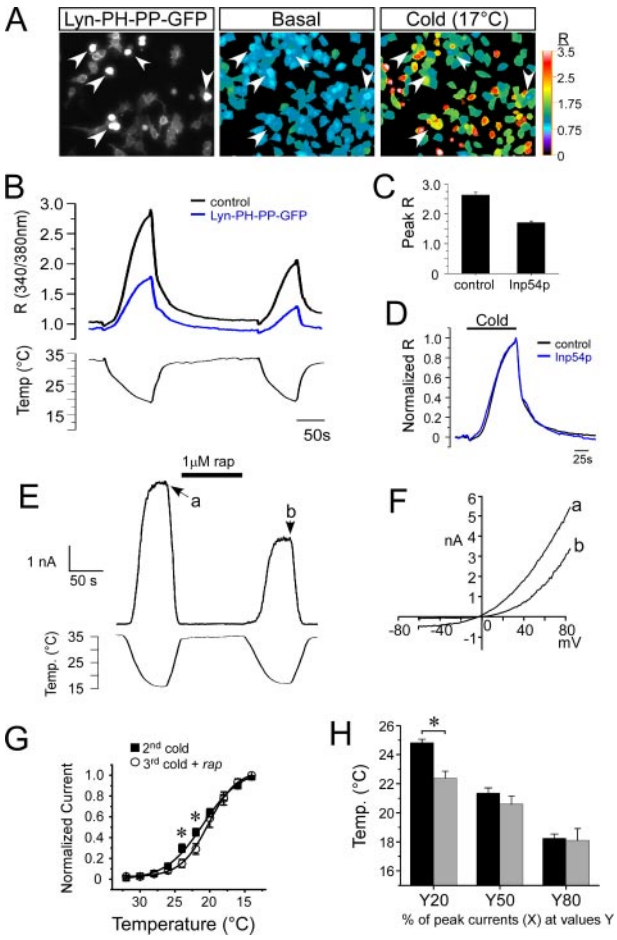

FIGURE 6. **PLC-independent depletion of plasmalemmal PIP_2 reduces cold-evoked TRPM8 currents but does not alter temperature sensitivity.** *A,* representative images of HEK293T cells expressing rTRPM8 and Lyn-PH-PP-GFP. *Left panel,* GFP fluorescence marks the cells expressing both constructs. *Middle* and *right panels,* pseudocolored images of the 340/380 nm Fura-2 ratio (*R*) show low basal Ca^{2+} when the perfusate is held at ~33 °C, but increased *R* values when perfusate temperature is reduced to 17 °C. *Arrowheads* mark GFP^+ cells expressing Lyn-PH-PP-GFP. *B,* averaged changes in the Fura-2 ratio taken from *A* of control TRPM8-expressing cells (*black lines*, n = 11 cells) *versus* those co-expressing Lyn-PH-PP-GFP (*blue lines*, n = 13 cells). *C,* peak *R* values for each condition. Data are represented as the average peak *R* values at 17 °C and are from seven independent experiments that averaged 11–25 cells per experiment. *D,* normalized Ca^{2+} responses to the 1st cold ramp shown in *B* for TRPM8-expressing cells and TRPM8 and Lyn-PH-PP-GFP co-expressing cells. The base-line *R* values were first subtracted and then each trace was normalized to the peak *R* value at 17 °C. *E,* representative whole-cell voltage clamp recording (holding potential (*h.p.*) +80 mV) from a cell transfected with rTRPM8, FKBP-Inp54p, and Lyn11-FRB. Cold-evoked TRPM8 currents were diminished following application of the dimerizing agent rapamycin (*rap*). *F,* representative current-voltage relationships for before and after Inp54p translocation to a cold stimulus (15 °C). Data are taken from the time points indicated in *E*. *G,* current to temperature relationship of TRPM8 responses before and after translocation of Inp54p to the plasma membrane by the dimerizer rapamycin. Cold-evoked TRPM8 currents (in the presence of 50 μM menthol) were normalized to a maximal saturating response at 14 °C (n = 6). There was a slight significant difference in the normalized current amplitudes at 24 and 22 °C ($p < 0.05$, *asterisks*). *H,* current to temperature relationships were plotted and fit with a sigmoidal relationship, and the temperature at 20 (*Y20*), 50 (*Y50*), and 80% (*Y80*) of the peak currents at 14 °C were calculated from the curve. At 20% of the peak current, there was a significant difference ($p < 0.05$) in the temperatures before and after Inp54p translocation, but not at 50 and 80%.

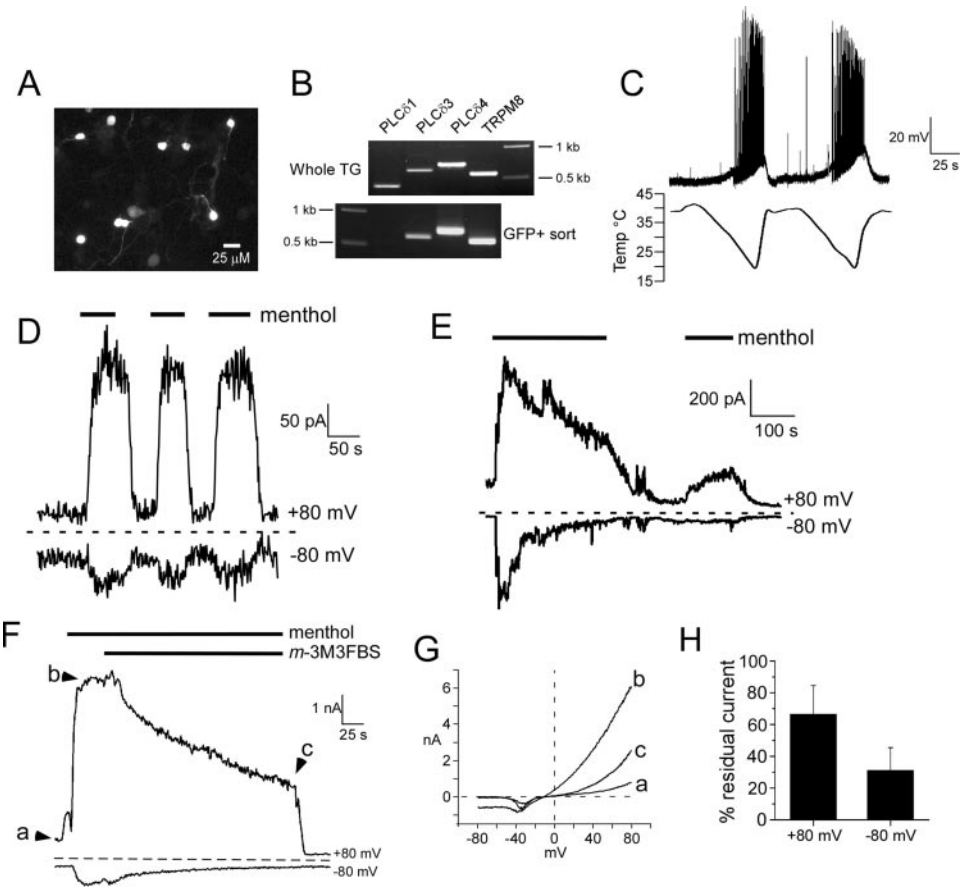

FIGURE 7. **Adaptation of neuronal TRPM8 currents is Ca^{2+}-dependent and mimicked by PLC activation.** *A,* fluorescent photomicrograph of cultured TG $TRPM8^+$ neurons visualized by GFP expression. *B,* representative RT-PCR DNA bands for expression of PLCδ isozymes in TRPM8 neurons *in vivo*. All three isozymes are present in whole TG tissue samples, whereas PLCδ3 and PLCδ4 predominate in TRPM8 neurons ($n = 3$ experiments). *C,* whole-cell current clamp recordings from a TRPM8-expressing neuron in which trains of action potentials were elicited by two successive cold pulses ($n = 5$). *D,* whole-cell menthol-evoked (200 μM) currents from TRPM8-expressing neurons do not adapt to repeated stimuli in the absence of external Ca^{2+} and with 5 mM EGTA in the recording pipette ($n = 5$). *E,* in the presence of physiological (2 mM) calcium and weak intracellular Ca^{2+} buffering (0.5 mM EGTA), whole-cell menthol-evoked neuronal currents adapt over time and do not recover fully on subsequent menthol exposures when the cell is held at 22 °C ($n = 6$). *F,* menthol-evoked currents in TRPM8 TG neurons decrease or adapt upon bath application of 5 μM *m*-3M3FBS ($n = 7$). *G,* current-voltage relations at the points indicated in *F*. *H,* average residual TRPM8 currents in neurons after application of 5 μM *m*-3M3FBS for 3 min. at both positive and negative potentials. *m*-3M3FBS reduces currents to 66.7 ± 17.9 and 31.2 ± 14.3% ($n = 7$) at positive and negative membrane potentials, respectively.

6*G*, the temperature dependence of cold-evoked currents before and after Inp54p translocation was largely unchanged. However, normalized currents at near threshold temperatures were slightly diminished after phosphatase translocation (at 24 °C, 0.30 ± 0.04 before and 0.15 ± 0.04 after translocation; at 22 °C, 0.45 ± 0.04 before and 0.29 ± 0.05 after translocation, $p < 0.05$ ($n = 7$); Fig. 6*G*). Temperature-response profiles were best fit with a sigmoidal relationship (Fig. 6*G*), allowing for the calculation of the average temperature at 20, 50, and 80% of the peak currents (at 14 °C). Using these analyses (Fig. 6*H*), we found limited but significant differences between before and after Inp54p translocation at the 20% value (24.8 ± 0.3 °C before and 22.2 ± 0.5 °C after translocation, $p < 0.05$ ($n = 7$)). However, no difference in temperature sensitivity was observed at other points along the temperature-response curve (Fig. 6*H*), demonstrating no overt change in channel sensitivity to cold after PIP_2 depletion.

Ca^{2+} Dependence of Native TRPM8 Currents in Neurons—Although heterologously expressed TRPM8 adapts to both cold and menthol stimuli, we sought to verify that native TRPM8 channels adapt in a like manner, taking advantage of a transgenic mouse line in which TRPM8 neurons express EGFP *in vivo* (6). This animal model provides significant benefits in that TRPM8-expressing neurons are identified without prior exposure to channel agonists, which may alter the state of adaptation or cell function. As shown in Fig. 7*A*, cultured neonatal mouse trigeminal ganglia neurons expressing TRPM8 are readily identifiable by GFP fluorescence (6). This robustness of GFP fluorescence also allowed us to determine the expression of the Ca^{2+}-sensitive PLCδ isozymes in TRPM8 neurons. GFP-positive dissociated TG neurons were purified by fluorescence-activated cell sorting (see supplemental Fig. 2*D*), and expression of TRPM8 neuron-specific PLCδ isozymes was determined by RT-PCR (see under "Experimental Procedures"). As shown in Fig. 7*B*, all three isozymes were detected in samples of whole trigeminal ganglia, although in 2 of 3 experiments only PLCδ3 and -4 were observed in purified TRPM8 neurons. Thus, these data demonstrate that TRPM8 neurons express Ca^{2+}-sensitive PLCδ isozymes.

We next characterized cold responsiveness of GFP^+ cells electrophysiologically first in current clamp mode to determine whether action potentials were evoked in these cells by cold stimuli (a cold ramp from 40 to 15 °C; Fig. 7*C*). GFP^+ neurons had an average resting membrane potential of −51.6 ± 4.8 mV ($n = 5$), and began to depolarize when the perfusate was cooled below 28.3 ± 1.4 °C. Cold-evoked action potential amplitudes were 76.4 ± 8.5 mV with durations at takeoff voltage of 5.1 ± 0.8 ms and after hyperpolarizations of 4.9 ± 1.7 mV. We observed the first action potentials at an average threshold temperature of 24.2 ± 1.6 °C, with a range of thresholds from 27.3 to 18 °C. These data are consistent with nerve recordings using the skin-nerve preparation in TRPM8-null mice that lack cold responses over a range of temperatures (9),[3] suggesting that the TRPM8 population of neurons is responsive to both innocuous and noxious cold temperatures *in vitro*.

[3] C. Stucky, personal communication.

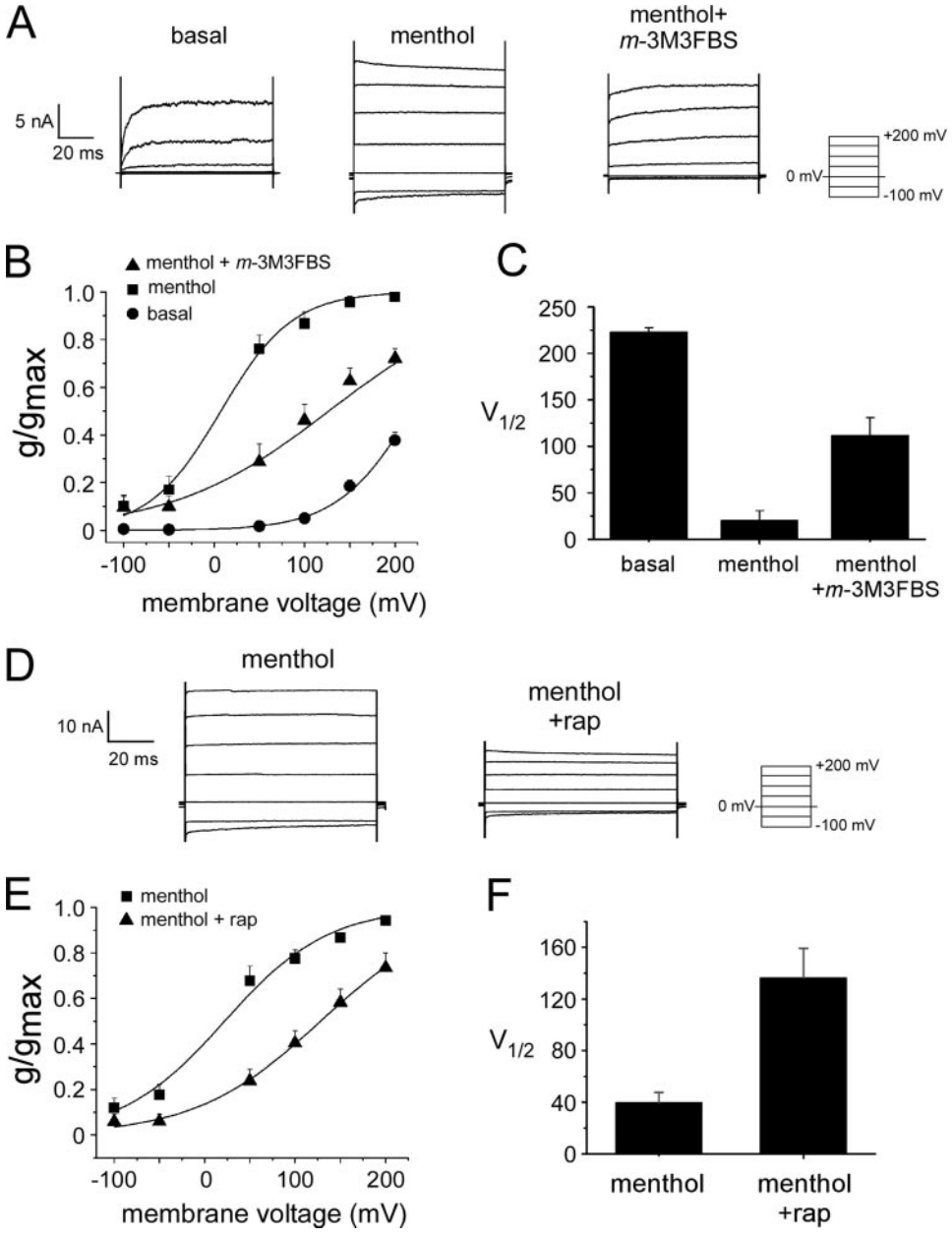

FIGURE 8. **PLC activation and PIP_2 depletion shifts the voltage dependence of TRPM8 channel gating.** *A,* representative whole-cell TRPM8 current traces in response to the indicated voltage protocol. Traces show activity before and after 1 mM menthol application, and after application of 5 μM *m*-3M3FBS (while still in the presence of 1 mM menthol). *B,* steady-state activation curves. The normalized conductance (g/g_{max}) was determined as explained under "Experimental Procedures." *Lines* represent Boltzmann functions fitted to the data ($n = 6$). *C,* average voltages of half-maximal g/g_{max} ($V_{1/2}$) obtained by fitting data to a Boltzmann function as described ($n = 6$). *D,* representative whole-cell TRPM8 current traces in response to the indicated voltage protocol. *Traces* show TRPM8 activation by 1 mM menthol, before and after Inp54p translocation induced by 1 μM rapamycin (*rap*). *E,* steady-state activation curves. *Lines* represent Boltzmann functions fitted to the data ($n = 12$). *F,* average voltage of half-maximal g/g_{max} ($V_{1/2}$), obtained by fitting data to a Boltzmann function ($n = 12$).

We have reported previously that menthol evokes outwardly rectifying currents in TRPM8-GFP neurons that adapt in the presence of Ca^{2+} (6). As shown in Fig. 7*D*, and like heterologously expressed channels, when menthol-evoked currents are recorded in nominally Ca^{2+}-free external solutions and with strong Ca^{2+} buffering in the pipette, menthol currents are sustained and do not exhibit adaptation. However, when Ca^{2+} is present externally and the recording pipette is weakly buffered for Ca^{2+}, menthol-evoked currents adapt over time (Fig. 7*E*). Thus, these data are consistent with previous reports and demonstrate that TRPM8 channels expressed both heterologously and in native afferent sensory neurons adapt in a Ca^{2+}-dependent manner.

Chemical Activation of PLC Reduces TRPM8 Currents in Neurons—Although it is clear that PLC activation adapts recombinant TRPM8 channels, it has not been demonstrated that native TRPM8 currents can be affected similarly. Thus, we extended our studies into native cells using the GFP transgenic mouse line (6). Similar to our results in heterologous cells, whole-cell neuronal currents evoked by 200 μM menthol are reduced upon application of 2.5 μM *m*-3M3FBS (Fig. 7, *F* and *G*). At positive potentials, the remaining currents were 66.7 ± 17.9% of peak currents, although at negative potentials, the remaining currents averaged 31.2 ± 14.3% ($n = 7$) (Fig. 7*H*). Thus, these data suggest that PLC is mediating TRPM8 adaptation in native cells, as well as in heterologous systems, and supports the hypothesis that TRPM8 is regulated downstream of PLC activity.

Adaptation Shifts the Voltage Dependence of TRPM8 Currents—TRPM8 exhibits voltage-dependent gating, and it has been demonstrated that menthol and cold shift the voltage dependence of the channel so that it opens more readily at physiological voltages (25, 26). Because adaptation is not a change in channel sensitivity to menthol or cold, we hypothesized that adaptation reflects a shift in channel voltage dependence toward more positive membrane voltages. We tested this hypothesis in heterologous cells by comparing TRPM8 conductances at steady-state holding potentials before and after we induced adaptation, either with *m*-3M3FBS-induced PLC activation or by 5′-phosphatase-mediated PIP_2 depletion (Fig. 8). The normalized TRPM8 conductance for each cell, referred to here as g/g_{max} (as in Refs. 25, 26), was plotted for the given voltages under basal conditions, after the application of 1 mM menthol, and after the addition of 5 μM *m*-3M3FBS (while still in the presence of 1 mM menthol) (Fig. 8*A*). The conductance to voltage relationship was fitted with a Boltzmann function, allowing the calculation of the half-

maximal activation voltage ($V_{½}$) under each condition. Using this protocol, we found that application of menthol shifted the activation curve toward negative membrane potentials (Fig. 8*B*), as has been reported previously (25). However, the reduction of TRPM8 currents by the application of *m*-3M3FBS, in the presence of menthol, shifts the curve back toward the basal state and more positive membrane potentials (Fig. 8*B*). The average $V_{½}$ values under basal conditions, after addition of menthol, and after addition of 5 μM *m*-3M3FBS were 223.0 ± 5.4, 20.5 ± 11.0, and 111.7 ± 21.1 mV, respectively (Fig. 8*C*). These results suggest that activation of PLC by *m*-3M3FBS alters TRPM8 by shifting the voltage dependence of channel gating toward more positive voltages, thereby reversing the effects of agonist activation.

One caveat for these results is that the by-products of PLC activation may be altering channel function. Therefore, we also tested the effect of adaptation using the rapamycin-induced translocation of Inp54p on the voltage dependence of TRPM8 gating (Fig. 8*D*). These experiments were performed in the same manner as described above. From the steady-state currents, we calculated conductances and fitted conductance-voltage relations to Boltzmann functions and estimated the $V_{½}$ value for each treatment condition (Fig. 8, *E* and *F*). In 12 of 12 cells tested, we found that the addition of rapamycin caused the activation curve to shift to more positive voltages. Specifically, we found that the average $V_{½}$ values upon menthol application and after addition of 1 μM rapamycin were 39.8 ± 8.1 and 136.5 ± 23.7 mV, respectively (Fig. 8*F*). Together, these findings suggest that TRPM8 activation and adaptation both reflect changes in the voltage dependence of channel gating.

DISCUSSION

Here we show that direct pharmacological activation of PLC reduces whole-cell recombinant TRPM8 currents, that PLC-independent PIP_2 depletion (without second messenger generation) reduces whole-cell recombinant TRPM8 currents, and that chemical activation of PLC reduces whole-cell TRPM8 currents in native cells. These data support the hypothesis that PLC regulates TRPM8 activity and underlies Ca^{2+}-mediated adaption to cold and cooling compounds such as menthol. In our investigation of TRPM8 adaption, we also show that the reduction in TRPM8 activity is not because of alterations in sensitivity of the channel to temperature or agonist, but is a result in a shift in voltage-dependent gating. Thus our results provide insights into how TRPM8 activity is mechanistically altered under adapting conditions.

Adaptation to cold stimuli occurs both *in vivo* and *in vitro* (13–15, 18, 39). Reid and co-workers (15, 18, 40), using cold- or menthol-sensitive cultured DRG neurons, found that either stimulus evokes ionic currents that rapidly adapt in a Ca^{2+}-dependent manner when recording in the whole-cell configuration. However, adaptation was absent when recordings were made from excised membrane patches, but a higher threshold temperature (*i.e.* colder temperature) of ~18 °C was required for activation (40). Similarly, we and others have shown that both menthol- and cold-evoked currents, in cells heterologously expressing TRPM8, adapt in an intracellular Ca^{2+}-dependent manner (7). Interestingly, adapted currents recover upon a return to physiologically warm temperatures, but will remain in this adapted state as long as the cell is held at sub-physiological temperatures (~22 °C; see Fig. 1). Moreover, we found that adaptation of TRPM8 was much more robust when the activating temperature is held at 15 *versus* 6 °C. These observations strongly suggest that adaptation is mediated, at least in part, by a temperature-dependent enzymatic process and are consistent with the PIP_2 model. PIP_2 levels are determined not only by PLC activity, but also by phosphoinositide synthesis enzymes, whose activities are likely temperature sensitive (30). In the case of the former, our observation that currents evoked by an extreme cold stimulus (~6 °C) adapt to a lesser extent than warmer stimuli (15 °C) may indicate that PLC hydrolysis of PIP_2 is slowed at colder temperatures. Similarly, under conditions as those shown in Fig. 1*E*, adapted currents will recover more slowly at cold temperatures because of cold inhibition of PIP_2 synthesis enzymes. Another consideration for the slowing of recovery at cold temperatures is that membrane fluidity is decreased as a result of cooling, thus perhaps slowing lateral diffusion of PIP_2 that is needed to replenish PIP_2 at TRPM8 channels.

This hypothesis is further supported by reports demonstrating that PIP_2 is an obligatory factor in TRPM8 function (16, 17). TRPM8 currents are remarkably stable in whole-cell recordings under Ca^{2+}-free conditions, yet rapidly rundown after membrane patch excision. Rundown could be inhibited if the patch was exposed to a mixture of phosphatase inhibitors, as well as enhanced in the presence of magnesium (16). The role of PIP_2 was inferred when it was shown that exposing the cytoplasmic surface of the patch to exogenous PIP_2 restored TRPM8 currents to pre-rundown levels (16, 17). Thus, it is clear that PIP_2 is important for TRPM8 function, and that any mechanism whereby plasmalemmal levels of the lipid are reduced would lead to decreased channel activity. As PLC and phosphoinositide kinases break down and synthesize PIP_2, respectively, either pathway is likely to regulate TRPM8 function.

This important role of PLC and PIP_2 in regulating TRPM8 is not surprising as this enzyme, and the resulting signaling cascade, is known to regulate several TRP channels via mechanisms that include the hydrolysis of PIP_2, production of lipid metabolites, or the release of Ca^{2+} from intracellular stores (41, 42). For example, the channel homologues TRPM4 and TRPM5 are keenly sensitive to PIP_2 (24, 43–45). TRPM5 is critical for coding of sweet, bitter, and umami tastants and is activated downstream of GPCR tastant receptors that are coupled to α-gustducin and PLCβ_2 (46, 47). Current models suggest that Ca^{2+} liberation from intracellular stores, via IP_3 synthesis from PIP_2 cleavage, are detected by TRPM5 and thereby lead to channel activation and neural signaling (24, 44, 47). A similar Ca^{2+}-mediated activation mechanism has also been postulated for TRPM4 activation (45). PIP_2 has also been shown to be involved in desensitization of TRPM4 and TRPM5 where it appears to play a partially obligatory role in the activity of each channel in very much the same manner as TRPM8 (16, 17, 24, 45).

In addition to TRPM4 and TRPM5, PIP_2 has also been shown to regulate activity of the heat- and capsaicin-gated ion channel TRPV1, although with an interesting duality of action (48).

Receptor-mediated hydrolysis of PIP_2 was initially suggested to sensitize TRPV1 to capsaicin, heat, and protons, by releasing an inhibitory effect of PIP_2 on the channel (49, 50). However, more recent evidence suggests that PIP_2 is an obligatory component of the protein complex, and its presence is likely required for normal channel function (48, 51–54). This dual regulatory role for PIP_2 on TRPV1 function has recently been proposed to be dependent on the degree of channel stimulation (48, 53). Thus, PIP_2 is a key and nearly ubiquitous regulator of TRP ion channel function in many biological systems.

Our results suggest adaptation is manifested as a change in TRPM8 voltage-dependent gating, which is antagonistic to the changes evoked by either temperature or agonist activation. This observation was consistent with adaptation evoked by either PLC activation or by PLC-independent dephosphorylation of PIP_2, suggesting a conserved mechanism for the shift in voltage dependence of the channel. Voltage dependence of TRPM8 has been proposed to be strongly linked to temperature sensitivity of the channel (25, 26). TRP ion channels are structurally similar to voltage-gated potassium (Kv) channels, and mutagenesis of positively charged residues within the S4 and S5 transmembrane domains have been shown to alter voltage dependence of TRPM8, as well as thermal and menthol sensitivity of the channel (26). However, our results are contradictory as a large change in the temperature sensitivity of TRPM8 was not observed when adaption was induced by either PLC activation or PIP_2 reduction, nor was the dose dependence of menthol in activating TRPM8 altered with PIP_2 depletion. Indeed, there is ample evidence that temperature-, agonist- and voltage-dependent activations of TRPM8 are almost completely independent processes (29, 55–57). Mutagenesis strategies have identified the existence of distinct activation domains for voltage, temperature, and PIP_2, suggesting that each works allosterically to gate TRPM8 (29). Our data are consistent with an allosteric model, and yet it remains an open question as to how activation of TRPM8, and other thermosensitive TRP channels, is coordinated by all three critical components.

It should be noted that other groups have proposed alternative mechanisms for TRPM8 adaptation. For example, adaptation has been reported to be the result of calcium-sensitive protein kinase C (PKC) activation (22, 23). In these studies, several PKC activators (phorbol myristate acetate and phorbol 12,12-dibutyrate) were demonstrated to reduce whole-cell TRPM8 currents. However no evidence of TRPM8 phosphorylation was found (although one group did report an unexpected decrease in TRPM8 phosphorylation (23)), and mutations in putative serine and threonine phosphorylation sites do not alter adaptation. Therefore, it remains unclear whether the reduction in TRPM8 currents by PKC activators is indeed through phosphorylation events or some other unspecified mechanism. However, it is entirely plausible that the two processes are indeed linked. For example, a product of PLC activation and PIP_2 hydrolysis is diacylglycerol (DAG), an activator of PKC. Thus, under conditions of high intracellular Ca^{2+} and production of DAG, as would occur if Ca^{2+} influx during menthol- or cold-evoked TRPM8 currents leads to activation of PLC, PKC activity will increase and potentially affect TRPM8 activity. Although they do not conclusively rule out a role of PKC in TRPM8 adaptation, our results with the PIP_2 phosphatase Inp54p suggest that adaptation does not require PKC activity.

An important implication of PLC activity in a neuron is that it may regulate TRPM8 activity, thereby modifying the sensitivity of the cell to thermal stimuli. We and others have previously demonstrated that TRPM8 neurons are a diverse and heterogeneous cell population, and share common features with nociceptive and non-nociceptive neurons (6, 58, 59). Therefore, it is plausible that PLC plays a role in regulating one or more sensory perceptions, including innocuous cool or painful cold. It has also been shown that TRPM8 functions in cooling-induced analgesia, and that cold-fiber activation appears to reduce pain-induced behaviors via glutamatergic activity in the spinal cord (12). Thus, TRPM8 plays a diverse and wide ranging role in cold sensation and provides for the detection of a broad range of perceived cold temperatures.

Our results suggest a cellular mechanism whereby the thermal sensitivity of TRPM8-expressing neurons can be altered or tuned by PIP_2 metabolism. For example, in neurons in which the ratio of PIP_2 synthesis to breakdown is high, cold stimuli will produce a large, robust depolarization of TRPM8-expressing neurons. Alternatively, if the synthesis-to-breakdown ratio is reduced such that PIP_2 levels are diminished, equivalent stimulus intensities will be less effective. Precedent for this hypothesis comes from recent work in cultured cold- and menthol-sensitive DRG neurons exposed to inflammatory mediators bradykinin, prostaglandin E_2, and histamine (60). The receptors for each of these substances are linked to PLC and neuronal exposure to these reduced cold and menthol responses, indirectly suggesting that PLC activity produced decreased TRPM8 activity as observed in this study. Thus, these data suggest that cold responsiveness is a highly dynamic process and that different cellular conditions can lead to altered thermal sensitivity by PLC-mediated modifications of TRPM8.

Acknowledgments—We thank the following individuals for their generous gifts of reagents: Drs. Tobias Meyer (Stanford University) and Mark Shapiro (University of Texas Health Science Center) for the EGFP-Lyn-PH-PP cDNA; Drs. Bertil Hille and Ken Mackie (University of Washington) for the PLCδ1-PH-RFP and PLCδ1-PH-YFP cDNAs; Drs. Emily Liman (University of Southern California), B. Hille, and T. Meyer for the rapamycin-inducible In54p system cDNA. We are indebted to Dr. Liman for her training and expertise in electrophysiology, as well as helpful discussion during the course of this study. We also thank Dr. David Julius (University of California, San Francisco) for advice and encouragement. Finally, we thank all members of the McKemy lab for their encouragement, advice, and assistance throughout this project.

REFERENCES

1. Julius, D., and Basbaum, A. I. (2001) *Nature* **413,** 203–210
2. Byers, M. R., and Narhi, M. V. O. (2002) in *Dental Pulp* (Hargreaves, K. M., and Goodis, H. E., eds) Vol. 3, pp. 151–179, Quintessence Publishing Co, Inc, Carol Stream, IL
3. Han, Z. S., Zhang, E. T., and Craig, A. D. (1998) *Nat. Neurosci.* **1,** 218–225
4. Jordt, S. E., McKemy, D. D., and Julius, D. (2003) *Curr. Opin. Neurobiol.* **13,** 487–492
5. Daniels, R. L., and McKemy, D. D. (2007) *Mol. Pain* **3,** 23
6. Takashima, Y., Daniels, R. L., Knowlton, W., Teng, J., Liman, E. R., and

McKemy, D. D. (2007) *J. Neurosci.* **27,** 14147–14157
7. McKemy, D. D., Neuhausser, W. M., and Julius, D. (2002) *Nature* **416,** 52–58
8. Peier, A. M., Moqrich, A., Hergarden, A. C., Reeve, A. J., Andersson, D. A., Story, G. M., Earley, T. J., Dragoni, I., McIntyre, P., Bevan, S., and Patapoutian, A. (2002) *Cell* **108,** 705–715
9. Bautista, D. M., Siemens, J., Glazer, J. M., Tsuruda, P. R., Basbaum, A. I., Stucky, C. L., Jordt, S. E., and Julius, D. (2007) *Nature* **448,** 204–208
10. Colburn, R. W., Lubin, M. L., Stone, D. J., Jr., Wang, Y., Lawrence, D., D'Andrea, M. R., Brandt, M. R., Liu, Y., Flores, C. M., and Qin, N. (2007) *Neuron* **54,** 379–386
11. Dhaka, A., Murray, A. N., Mathur, J., Earley, T. J., Petrus, M. J., and Patapoutian, A. (2007) *Neuron* **54,** 371–378
12. Proudfoot, C. J., Garry, E. M., Cottrell, D. F., Rosie, R., Anderson, H., Robertson, D. C., Fleetwood-Walker, S. M., and Mitchell, R. (2006) *Curr. Biol.* **16,** 1591–1605
13. Campero, M., Serra, J., Bostock, H., and Ochoa, J. L. (2001) *J. Physiol.* (*Lond.*) **535,** 855–865
14. Darian-Smith, I., Johnson, K. O., and Dykes, R. (1973) *J. Neurophysiol.* **36,** 325–346
15. Reid, G., and Flonta, M. L. (2001) *Nature* **413,** 480
16. Liu, B., and Qin, F. (2005) *J. Neurosci.* **25,** 1674–1681
17. Rohacs, T., Lopes, C. M., Michailidis, I., and Logothetis, D. E. (2005) *Nat. Neurosci.* **8,** 626–634
18. Reid, G., Babes, A., and Pluteanu, F. (2002) *J. Physiol.* (*Lond.*) **545,** 595–614
19. Rohacs, T. (2007) *Pfluegers Arch.* **453,** 753–762
20. Rohacs, T., and Nilius, B. (2007) *Pfluegers Arch.* **455,** 157–168
21. Rebecchi, M. J., and Pentyala, S. N. (2000) *Physiol. Rev.* **80,** 1291–1335
22. Abe, J., Hosokawa, H., Sawada, Y., Matsumura, K., and Kobayashi, S. (2006) *Neurosci. Lett.* **397,** 140–144
23. Premkumar, L. S., Raisinghani, M., Pingle, S. C., Long, C., and Pimentel, F. (2005) *J. Neurosci.* **25,** 11322–11329
24. Liu, D., and Liman, E. R. (2003) *Proc. Natl. Acad. Sci. U. S. A.* **100,** 15160–15165
25. Voets, T., Droogmans, G., Wissenbach, U., Janssens, A., Flockerzi, V., and Nilius, B. (2004) *Nature* **430,** 748–754
26. Voets, T., Owsianik, G., Janssens, A., Talavera, K., and Nilius, B. (2007) *Nat. Chem. Biol.* **3,** 174–182
27. Jordt, S. E., Bautista, D. M., Chuang, H. H., McKemy, D. D., Zygmunt, P. M., Hogestatt, E. D., Meng, I. D., and Julius, D. (2004) *Nature* **427,** 260–265
28. Hui, K., Guo, Y., and Feng, Z. P. (2005) *Biochem. Biophys. Res. Commun.* **333,** 374–382
29. Brauchi, S., Orta, G., Mascayano, C., Salazar, M., Raddatz, N., Urbina, H., Rosenmann, E., Gonzalez-Nilo, F., and Latorre, R. (2007) *Proc. Natl. Acad. Sci. U. S. A.* **104,** 10246–10251
30. Horowitz, L. F., Hirdes, W., Suh, B. C., Hilgemann, D. W., Mackie, K., and Hille, B. (2005) *J. Gen. Physiol.* **126,** 243–262
31. Bae, Y. S., Lee, T. G., Park, J. C., Hur, J. H., Kim, Y., Heo, K., Kwak, J. Y., Suh, P. G., and Ryu, S. H. (2003) *Mol. Pharmacol.* **63,** 1043–1050
32. Nam, J. H., Lee, H.-S., Nguyen, Y. H., Kang, T. M., Lee, S. W., Kim, H.-Y., Kim, S. J., Earm, Y. E., and Kim, S. J. (2007) *J. Physiol.* (*Lond.*) **582,** 977–990
33. Jajoo, S., Mukherjea, D., Brewer, G. J., and Ramkumar, V. (2008) *Neuroscience* **151,** 525–532
34. Zufall, F., and Leinders-Zufall, T. (2000) *Chem. Senses* **25,** 473–481
35. Raucher, D., Stauffer, T., Chen, W., Shen, K., Guo, S., York, J. D., Sheetz, M. P., and Meyer, T. (2000) *Cell* **100,** 221–228
36. Li, Y., Gamper, N., Hilgemann, D. W., and Shapiro, M. S. (2005) *J. Neurosci.* **25,** 9825–9835
37. Suh, B. C., Inoue, T., Meyer, T., and Hille, B. (2006) *Science* **314,** 1454–1457
38. Varnai, P., Thyagarajan, B., Rohacs, T., and Balla, T. (2006) *J. Cell Biol.* **175,** 377–382
39. Kenshalo, D. R., and Duclaux, R. (1977) *J. Neurophysiol.* **40,** 319–332
40. Reid, G., and Flonta, M. L. (2002) *Neurosci. Lett.* **324,** 164–168
41. Montell, C., Birnbaumer, L., and Flockerzi, V. (2002) *Cell* **108,** 595–598
42. Clapham, D. E. (2003) *Nature* **426,** 517–524
43. Hofmann, T., Chubanov, V., Gudermann, T., and Montell, C. (2003) *Curr. Biol.* **13,** 1153–1158
44. Prawitt, D., Monteilh-Zoller, M. K., Brixel, L., Spangenberg, C., Zabel, B., Fleig, A., and Penner, R. (2003) *Proc. Natl. Acad. Sci. U. S. A.* **100,** 15166–15171
45. Zhang, Z., Okawa, H., Wang, Y., and Liman, E. R. (2005) *J. Biol. Chem.* **280,** 39185–39192
46. Zhang, Y., Hoon, M. A., Chandrashekar, J., Mueller, K. L., Cook, B., Wu, D., Zuker, C. S., and Ryba, N. J. (2003) *Cell* **112,** 293–301
47. Perez, C. A., Huang, L., Rong, M., Kozak, J. A., Preuss, A. K., Zhang, H., Max, M., and Margolskee, R. F. (2002) *Nat. Neurosci.* **5,** 1169–1176
48. Rohacs, T., Thyagarajan, B., and Lukas, V. (2008) *Mol. Neurobiol.* **37,** 153–163
49. Chuang, H. H., Prescott, E. D., Kong, H., Shields, S., Jordt, S. E., Basbaum, A. I., Chao, M. V., and Julius, D. (2001) *Nature* **411,** 957–962
50. Prescott, E. D., and Julius, D. (2003) *Science* **300,** 1284–1288
51. Lishko, P. V., Procko, E., Jin, X., Phelps, C. B., and Gaudet, R. (2007) *Neuron* **54,** 905–918
52. Liu, B., Zhang, C., and Qin, F. (2005) *J. Neurosci.* **25,** 4835–4843
53. Lukacs, V., Thyagarajan, B., Varnai, P., Balla, A., Balla, T., and Rohacs, T. (2007) *J. Neurosci.* **27,** 7070–7080
54. Klein, R. M., Ufret-Vincenty, C. A., Hua, L., and Gordon, S. E. (2008) *J. Biol. Chem.* **283,** 26208–26216
55. Matta, J. A., and Ahern, G. P. (2007) *J. Physiol.* (*Lond.*) **585,** 469–482
56. Brauchi, S., Orio, P., and Latorre, R. (2004) *Proc. Natl. Acad. Sci. U. S. A.* **101,** 15494–15499
57. Brauchi, S., Orta, G., Salazar, M., Rosenmann, E., and Latorre, R. (2006) *J. Neurosci.* **26,** 4835–4840
58. Xing, H., Ling, J., Chen, M., and Gu, J. G. (2006) *J. Neurophysiol.* **95,** 1221–1230
59. Dhaka, A., Earley, T. J., Watson, J., and Patapoutian, A. (2008) *J. Neurosci.* **28,** 566–575
60. Linte, R. M., Ciobanu, C., Reid, G., and Babes, A. (2007) *Exp. Brain Res.* **178,** 89–98